

omit all  $U_h'$  with an absolute value less than 0.1 without any serious influence on the resolution of the atomic positions by computation of the electron density function.

Table 1. Number of unitary structure factors  $U_h'$  determined in sign by application of probability relation (10)

Only reflexions without contribution of heavy atoms are involved.

$U_h'$	Number of reflexions	Number of correct signs (%)
0.00-0.05	33	69.7
0.05-0.10	82	71.5
0.10-0.15	67	81.3
0.15-0.20	32	90.6
0.20-0.25	9	100.0
0.25-0.30	8	100.0

The presence of further heavy atoms in the structure influences the probability  $P_+$  unfavourably. We can compare the structure of  $\text{Cu}_2\text{C}_{24}\text{N}_{12}\text{O}_{12}\text{H}_{56}$  considered above with the structure of  $\text{Cu}_2\text{C}_8\text{N}_{12}\text{O}_{16}\text{H}_{28}\text{K}_2$  (Freeman, Smith & Taylor, 1961). Both  $F(000)=422$  and  $2n_{\text{Cu}}=0.178$  of the latter structure are comparable to corresponding values of the first structure, but the value of  $\varepsilon$  differs considerably ( $\varepsilon=0.0097$ ). The fraction of structure factors determined in sign by the presence

of heavy atoms in special positions is 89.7%. The theoretical value is 90.4%.

The method described in this paper is sufficiently effective for a complete solution of the phase problem in the case of a structure with heavy atoms in special positions. The only condition is a high probability  $P_+$  for reflexions with a contribution from the heavy atoms. This may be tested by relations (4) and (7) before starting the structure determination.

I am very indebted to Professor M. A. Porai-Koshits for suggesting the possibility of using equation (22).

I wish to thank Miss O. Šalyová for her assistance with the computations.

#### References

- FREEMAN, H. C., SMITH, J. E. W. L. & TAYLOR, J. C. (1961). *Acta Cryst.* **14**, 407.  
 HANIC, F. & SERATOR, M. (1964). *Chemické Zvesti*, **18**, 572.  
 LUZZATI, V. (1953). *Acta Cryst.* **6**, 142.  
 SIM, G. A. (1957). *Acta Cryst.* **10**, 177.  
 WILSON, A. J. C. (1949). *Acta Cryst.* **2**, 318.  
 WOOLFSON, M. M. (1956). *Acta Cryst.* **9**, 804.  
 WOOLFSON, M. M. (1961). *Direct Methods in Crystallography*, p. 55. Oxford: Clarendon Press.

*Acta Cryst.* (1966). **20**, 107

## The Crystal Structure of Triphenylmethylphosphonium Bis(1,2-dicyanoethylene-1,2-dithiolato)nickelate(III)\*

BY CHARLES J. FRITCHIE, JR.†

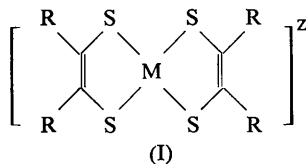
Central Research Department, Experimental Station, E. I. du Pont de Nemours and Company, Wilmington, Delaware, U.S.A.

(Received 29 December 1964 and in revised form 7 April 1965)

$\text{PCH}_3(\text{C}_6\text{H}_5)_3^+ \text{Ni}[\text{S}_2\text{C}_2(\text{CN})_2]_2^-$  crystallizes as a checkerboard arrangement of cationic and anionic columns, the latter containing ions of nearly  $D_{2h}$  symmetry essentially identical in dimensions with the isostructural dinegative ions. The anion radicals are so packed that spin-spin coupling through intermediacy of sulfur ( $\text{Ni} \cdots \text{S} = 3.59 \text{ \AA}$ ) rather than direct Ni-Ni bonding ( $\text{Ni} \cdots \text{Ni} \geq 4.40 \text{ \AA}$ ) is presumably responsible for the low magnetic moment. Average lengths of  $2.146 \pm 0.001 \text{ \AA}$  for Ni-S bonds and  $1.714 \pm 0.004 \text{ \AA}$  for S-C bonds suggest that sulfur is  $sp^2$  hybridized and involved in multiple bonding to the metal. The cationic column has a spine of face-to-face phenyl rings with projecting  $\text{PCH}_3(\text{C}_6\text{H}_5)_2$  side groups. P-C<sub>phenyl</sub> bonds average  $1.799 \text{ \AA}$ , somewhat shorter than the few previous reference values.

#### Introduction

The thiocoordinate chelates of generic formula (I)



\* Contribution No. 1050.

† Present address: Department of Chemistry, Tulane University, New Orleans, La., U.S.A.

have a number of unusual characteristics. The metal atom (M) can appear in unfamiliar valence states, and a given chelate can have various total charges. Bis(1,2-dicyanoethylene-1,2-dithiolato)nickel, for example, has been prepared having a total charge of  $z=0, 1-$ , or  $2-$ , and having nickel in formal oxidation states IV, III, or II. In addition, residual electron spins of paramagnetic chelates are often strongly coupled in the solid state. The nickel complex  $\text{Ni}[\text{S}_2\text{C}_2(\text{CN})_2]_2^-$  especially shows a high degree of spin-spin coupling, its tetraethylammonium salt having a magnetic moment

of 1.0 B.M. (Davison, Edelstein, Holm & Maki, 1963) and its triphenylmethylphosphonium salt one of 0.79 B.M. (Weiher, Melby & Benson, 1964). The latter compound was chosen for a diffraction study to ascertain the gross molecular geometry of the chelate, to study its bond lengths and angles, and to shed light on the nature of the intermolecular magnetic interaction.

### Experimental

The crystals used for this study are glistening black needles or tablets. Attempts to cut them usually resulted in fracturing or shattering of the sample. Some of the more equidimensional crystals were therefore used in their natal state for intensity measurements. Preliminary Weissenberg photographs showed the crystals to be triclinic; a primitive unit cell was chosen with the parameters  $a = 12.815 \pm 0.003$ ,  $b = 8.409 \pm 0.002$ ,  $c = 14.276 \pm 0.003$  Å,  $\alpha = 108.78 \pm 0.01^\circ$ ,  $\beta = 102.14 \pm 0.01^\circ$ , and  $\gamma = 93.93 \pm 0.01^\circ$ . On the basis of a satisfactorily refined model the salt is considered to have the symmetry of space group  $P\bar{1}$  ( $C_i$ ).

The unit-cell parameters were obtained from three zero-layer Weissenberg photographs of different crystals, two made on Supper equi-inclination instruments and calibrated with silicon powder and the third made with a camera designed solely for unit-cell measurement. The latter camera is approximately 100 mm in diameter, has the film wrapped around the outside rather than the inside of a cylinder for greater control of curvature, and utilizes the Straumanis geometry for effective radius determination. Each Weissenberg film yielded  $20\text{--}30 \sin^2 \theta$  values for resolved  $\text{Cu } K\alpha_1 - K\alpha_2$  doublets which were used in a least-squares procedure to obtain two distances and an angle characterizing that particular film. Lack of errors systematic in  $2\theta$ , over a range of about  $40^\circ$ , showed extrapolation to be unnecessary. The standard deviations quoted above are based upon standard analysis of the error of fit and upon the uncertainty in film radius. Pairs of  $d^*$  values measured on different films agree within the error limits given. Wavelengths used were  $\text{Cu } K\alpha_1 = 1.54050$  Å and  $\text{Cu } K\alpha_2 = 1.54434$  Å. The silicon powder is that used in the I.U.Cr. lattice constant project (Parrish, 1960) and has  $a = 5.4305$  Å.

The density of  $1.453 \pm 0.002$  g.cm<sup>-3</sup> calculated from the above unit cell and assuming  $Z=2$  agrees fairly well with the value of  $1.44 \pm 0.01$  g.cm<sup>-3</sup> measured by flotation in a zinc chloride solution. The latter value is of comparatively limited accuracy because of difficulty in wetting the crystals with the solution.

The majority of intensity data were estimated visually from a set of  $hkl$  Weissenberg photographs ( $n=0\text{--}7$ ) prepared with crystals about 0.1 mm in diameter using the multiple-film equi-inclination technique and  $\text{Cu } K\alpha$  radiation. These data were correlated after application of the appropriate Lorentz and polarization factors with a similar set of data from an [011] zero-layer photograph and with a group of 150 reflections meas-

ured on a Picker diffractometer, using a General Electric goniostat for orienting the crystal. Reflections with moderate, nearly equal intensities and scattering angles, but widely different  $\varphi$  settings, were chosen for this latter set. Analysis of random errors among the various measurements gave a mean  $R'$  value ( $R' = \Sigma |F_o - \bar{F}_o| / \Sigma |F_o|$ ) of 5%. Such a value ignores absorption and other systematic errors, giving only an estimate of the reproducibility of measurement. No absorption corrections were applied to the data. These errors are estimated to be less than 15% in  $|F_o|$  and on the average about 5%. A total of 5146 reflections were used in the calculations; the intensities of 1162 of these were indistinguishable from background in their respective positions of measurement and were considered to be less than these 'minimum observable values'.

### Trial structure and refinement

The nickel and sulfur positions were easily found by interpretation of the [010] and [011] Patterson projections; successive approximations to the electron densities in these projections, initiated with phases given by these atoms and refined by continually adding lighter atoms to the trial model gave a reasonably accurate picture of the molecular structure before use of three-dimensional data began. When the trial structure based on these projections included all atoms (except hydrogen) and was refined by least squares to  $R$  values near 20%, the then available three-dimensional data  $h1l$  through  $h3l$  were also used to improve the model. The  $R$  value for this sample of data dropped in 3 cycles from an initial value of  $\sim 30\%$  to 16.3%. Refinement continued when all the data were available, with the over-all  $R$  value dropping rapidly from an initial 28%.

Anisotropic (ellipsoidal) thermal parameters were introduced for the Ni, S, and P atoms when  $R$  was 18%; three cycles lowered  $R$  to 13%. A three-dimensional difference map was then computed to assess the validity of extending anisotropic thermal refinement to the lighter atoms in the presence of absorption errors not altogether negligible. The map showed anisotropic vibrational patterns for molecular groups which seemed physically reasonable. Extending anisotropic refinement to the carbon and nitrogen atoms lowered  $R$  to 10.5% in four cycles. A second difference map was then computed to locate hydrogen atoms and any possible irregularities in electron density. Well-defined peaks of  $0.3\text{--}0.7$  e.Å<sup>-3</sup> were found in reasonable positions for all hydrogen atoms; the only other dips or peaks greater than  $0.2$  e.Å<sup>-3</sup> occurred as streaks near the heaviest atoms and parallel to  $\mathbf{b}$ . These are attributed to a small scaling error in the  $h0l$  data which was subsequently eliminated. Addition of the 18 hydrogen atoms to the model, putting the methyl hydrogen atoms at peak positions and the remainder  $1.0$  Å from appropriate carbons, lowered  $R$  by 0.4%. A temperature factor of  $4.0$  Å<sup>2</sup> was used for all hydrogen atoms; neither this nor hydrogen positions were refined.

Table 1. *Final heavy-atom parameters and their standard deviations*

All figures have been multiplied by  $10^4$ .  
The temperature factor is of the form  $\exp \{-[B_{11}h^2 + B_{22}k^2 + B_{33}l^2 + B_{12}hk + B_{13}hl + B_{23}kl]\}$ .

Atom	<i>x</i>	<i>y</i>	<i>z</i>	$B_{11}$	$B_{22}$	$B_{33}$	$B_{12}$	$B_{13}$	$B_{23}$
Ni(1)	362 (1)	2358 (1)	-301 (1)	62 (1)	152 (2)	50 (1)	33 (1)	33 (1)	63 (2)
S(2)	1910 (1)	3817 (2)	-13 (1)	73 (1)	196 (3)	54 (1)	-13 (3)	35 (2)	38 (3)
S(3)	-1211 (1)	930 (2)	-653 (1)	63 (1)	192 (3)	71 (1)	42 (3)	55 (2)	83 (3)
S(4)	83 (1)	3929 (2)	1120 (1)	82 (1)	187 (3)	56 (1)	64 (3)	52 (2)	73 (3)
S(5)	696 (1)	775 (2)	-1681 (1)	65 (1)	184 (3)	59 (1)	-15 (3)	49 (2)	36 (3)
P(6)	3182 (1)	-1974 (2)	-3607 (1)	56 (1)	147 (3)	52 (1)	-2 (2)	21 (1)	58 (2)
N(7)	3822 (6)	7368 (11)	1840 (5)	106 (6)	314 (18)	79 (5)	-68 (16)	14 (9)	11 (14)
N(8)	1421 (7)	7586 (11)	3447 (5)	152 (8)	313 (18)	60 (4)	99 (20)	47 (9)	15 (14)
N(9)	-0460 (7)	-2993 (12)	-3951 (6)	124 (7)	348 (20)	87 (5)	-95 (19)	75 (10)	-50 (16)
N(10)	-2916 (5)	-2981 (9)	-2609 (5)	62 (4)	249 (15)	103 (5)	-1 (11)	29 (7)	112 (14)
C(11)	3029 (6)	6478 (10)	1556 (5)	81 (5)	209 (15)	60 (4)	17 (13)	17 (7)	66 (12)
C(12)	2033 (6)	5336 (8)	1165 (5)	82 (5)	157 (12)	48 (4)	20 (11)	12 (7)	63 (10)
C(13)	1238 (6)	5384 (8)	1658 (5)	96 (5)	136 (12)	47 (4)	67 (12)	21 (7)	58 (9)
C(14)	1342 (7)	6616 (10)	2647 (5)	104 (6)	210 (15)	50 (4)	81 (15)	25 (8)	63 (11)
C(15)	-0466 (6)	-1982 (10)	-3185 (6)	75 (5)	224 (16)	74 (5)	-35 (14)	53 (8)	22 (13)
C(16)	-0444 (5)	-0689 (8)	-2245 (5)	66 (4)	163 (12)	55 (4)	11 (10)	34 (6)	68 (10)
C(17)	-1281 (5)	-0632 (8)	-1794 (5)	55 (4)	146 (11)	65 (4)	24 (9)	24 (6)	90 (10)
C(18)	-2206 (5)	-1933 (9)	-2247 (5)	51 (4)	185 (13)	83 (5)	16 (10)	28 (7)	115 (12)
C(19)	2086 (6)	-3638 (10)	-4335 (6)	89 (6)	179 (14)	78 (5)	-33 (14)	0 (8)	83 (13)
C(20)	3697 (5)	-2186 (8)	-2385 (5)	66 (4)	158 (12)	58 (4)	30 (10)	46 (6)	76 (10)
C(21)	4715 (5)	-2604 (9)	-2123 (5)	75 (5)	193 (14)	60 (4)	63 (12)	49 (7)	80 (11)
C(22)	5092 (7)	-2674 (12)	-1182 (6)	80 (6)	313 (21)	76 (5)	82 (17)	27 (9)	139 (17)
C(23)	4453 (7)	-2507 (12)	-0502 (6)	115 (7)	332 (22)	53 (4)	97 (19)	42 (9)	131 (15)
C(24)	3436 (8)	-2116 (14)	-0759 (7)	126 (8)	366 (23)	74 (5)	149 (22)	108 (11)	171 (18)
C(25)	3042 (7)	-1955 (12)	-1706 (6)	91 (6)	308 (20)	81 (5)	126 (17)	88 (9)	162 (17)
C(26)	4222 (5)	-2094 (8)	-4288 (5)	69 (4)	148 (11)	54 (4)	33 (10)	38 (6)	73 (9)
C(27)	4091 (7)	-3327 (9)	-5232 (5)	114 (7)	169 (14)	56 (4)	50 (14)	50 (8)	63 (11)
C(28)	4911 (8)	-3370 (11)	-5724 (6)	145 (9)	229 (17)	70 (5)	142 (19)	115 (11)	80 (14)
C(29)	5866 (7)	-2252 (11)	-5282 (7)	115 (7)	265 (19)	107 (7)	143 (18)	136 (11)	209 (18)
C(30)	5977 (6)	-1001 (11)	-4343 (6)	87 (6)	252 (18)	92 (6)	47 (16)	74 (9)	162 (17)
C(31)	5151 (6)	-0924 (9)	-3844 (5)	74 (5)	194 (14)	63 (4)	12 (12)	38 (7)	87 (12)
C(32)	2696 (5)	0043 (8)	-3373 (5)	56 (4)	182 (12)	52 (3)	16 (10)	36 (6)	66 (10)
C(33)	1774 (6)	0215 (10)	-4026 (5)	73 (5)	228 (15)	68 (4)	71 (13)	36 (7)	115 (13)
C(34)	1428 (7)	1774 (12)	-3830 (7)	100 (7)	307 (21)	95 (6)	147 (19)	66 (10)	192 (19)
C(35)	1976 (8)	3157 (11)	-2985 (7)	134 (8)	196 (17)	115 (7)	138 (18)	143 (13)	175 (17)
C(36)	2883 (8)	2995 (10)	-2359 (7)	129 (8)	158 (15)	95 (6)	3 (16)	112 (12)	41 (14)
C(37)	3255 (6)	1439 (9)	-2539 (5)	70 (5)	174 (13)	73 (5)	16 (12)	41 (7)	48 (12)

Table 2. *Final hydrogen positional parameters*

Atom	<i>x</i>	<i>y</i>	<i>z</i>
H(38)	0.514	-0.277	-0.260
H(39)	0.579	-0.304	-0.100
H(40)	0.471	-0.262	0.014
H(41)	0.300	-0.192	-0.028
H(42)	0.236	-0.166	-0.188
H(43)	0.343	-0.415	-0.555
H(44)	0.484	-0.418	-0.637
H(45)	0.641	-0.228	-0.563
H(46)	0.665	-0.017	-0.403
H(47)	0.523	-0.014	-0.321
H(48)	0.138	-0.076	-0.462
H(49)	0.081	0.190	-0.427
H(50)	0.173	0.422	-0.287
H(51)	0.329	0.397	-0.175
H(52)	0.386	0.131	-0.210
H(53)	0.227	-0.471	-0.437
H(54)	0.180	-0.375	-0.503
H(55)	0.148	-0.342	-0.390

Two further least-squares cycles brought refinement to completion. The *R* value dropped by only 0.1% on the last cycle, to 9.0%. The average parameter shift was about 0.2  $\sigma$  and the largest 0.9  $\sigma$ . One further cycle was run with the 24 strongest reflections (which are serious-

ly reduced by extinction) removed. The *R* value for this list was 8.4%, but no parameter shifted by more than 0.3  $\sigma$ . The final parameters listed in Table 1 are those from the last cycle with all data. The figures in parentheses are standard deviations given by  $\sigma_m = 1.2 [A_{mn}^{-1} \sum w |F_o - F_c|^2 / (n-s)]^{1/2}$ , where all symbols have their usual meanings. The factor 1.2 is introduced as an empirical allowance for the use of a partially diagonalized matrix ( $9 \times 9$  one-atom blocks) in calculation of the inverse matrix elements  $A_{mn}^{-1}$ . The hydrogen positions are given in Table 2. Final values of  $|F_o|$  and  $|F_c|$  are listed in Table 3.

For all least-squares calculations a modification of the Gantzel-Sparks-Trueblood block-diagonal least-squares program, which minimizes  $\sum w |F_o - F_c|^2$ , was used. The subroutine for extraction of thermal-ellipsoid principal axes is one written by R. Deverill (private communication). Fourier summation and other programs were those of the author. Computations were performed on IBM 7090 and 7040 machines. The weighting scheme used in refinement was  $1/w = 1$  until *R* dropped to 20% and  $1/w = 1/(0.284 + 0.037|F_o|)$  thereafter. The latter function is the reciprocal of a straight



Table 3 (cont.)

A large table with multiple columns and rows of numerical data, including integers and negative values, organized in a grid-like structure.



Table 3 (cont.)

A large table with multiple columns of numbers, organized into several vertical sections. The numbers are arranged in a grid-like pattern, with some rows and columns containing specific identifiers or groupings. The data appears to be a continuation of a larger dataset or a specific calculation table.

Table 3 (cont.)

-4	79	-88	-6	68	-67	1	46	50	2	52	59	-2	-31	24	3	52	54	14	2	-11	37	-37	2	35	-35	15	-1		
-5	138	-147	-7	59	-40	2	-20	1	3	63	48	-3	41	-48	4	74	71	-2	68	-76	14	-2	3	46	-46	1	52	-17	
-6	129	-137	-8	85	73	-7	131	-112	4	129	130	-4	87	-82	0	33	30	0	111	0	0	22	-29	0	22	-29	3	17	25
-7	144	-159	-9	52	-55	-1	44	47	5	74	84	-5	98	-104	-1	33	27	-7	-28	-22	2	114	108	-1	46	54	-2	127	-124
-8	57	-66	-10	-31	8	-2	-28	-21	6	94	88	-6	-28	-31	-2	72	71	-8	-26	24	3	79	61	-2	48	60	-3	100	-107
-9	13	6	-11	85	70	-5	-28	-27	7	81	70	-7	79	89	-3	28	30	-9	-26	1	4	-24	15	3	92	101	-4	20	-12

line best fitting a plot of r.m.s.  $|\Delta F|$  versus  $|F_o|$ , constructed with data estimated on more than one film or both on film and by counter. The final value of  $[\sum w|F_o - F_c|^2/(n-s)]^{1/2}$  is 2.08 rather than unity, the difference probably being due to such factors as extinction and absorption which are not reflected in the weighting scheme.

Form factors used in all calculations are those in *International Tables for X-ray Crystallography* for Ni(III), S<sup>-</sup>, and P (all corrected for the real part of anomalous scattering), and those given by McWeeny (1951) for H, Freeman (1959) for N, and Hoerni & Ibers (1954) for C.

Discussion

Intramolecular structure

The present investigation, in correlation with a recent study of  $[N(CH_3)_4]^+ [Ni(S_2C_2(CN)_2)]^{2-}$  (Eisenberg, Ibers, Clark & Gray, 1964; hereafter EICG) represents the first case in which two oxidation states of a single molecular species have been studied by X-ray diffraction, and it is thus particularly interesting to compare the two. In both cases the chelate anion is approximately planar and very nearly has  $D_{2h}$  symmetry. The distortions from planarity in the present case can be described as a small tetrahedral buckling by the sulfur atoms and a further slight folding toward the cyano groups. Table 4 gives the least-squares plane of the chelate as a whole, as well as those of the largest planar fragments, the dicyanoethylene groups. Individual bond distances and angles within the anion are given in Fig. 1. Average parameters, under  $D_{2h}$  symmetry, are compared with corresponding values from EICG in Table 5. The two oxidation states probably have identical geometries, although differences in C=C

and C-S bond lengths are marginally significant. EICG's preliminary molecular orbital calculations indicate that the single electron by which the ions differ is located primarily on the nickel atom. If this is correct, no differences in ligand bond lengths are expected.

Table 4. Various least-squares planes through the anion with deviations  $\Delta$  and contributing weights  $w$

The planes are described in terms of an orthonormal coordinate system {M, N, P} with  $N||b$  and  $P||c^*$ .

Plane 1:  $-0.31614m + 0.82856n - 0.46210p = 1.7062$

Plane 2:  $-0.32444m + 0.84735n - 0.42039p = 1.8448$

Plane 3:  $-0.32754m + 0.79804n - 0.50581p = 1.8389$

Atom	$\Delta_1$	$w_1$	$\Delta_2$	$w_2$	$\Delta_3$	$w_3$
Ni(1)	0.029 Å	28	-0.091	0	-0.156	0
S(2)	0.054	16	-0.049	0		
S(3)	0.094	16			-0.022	0
S(4)	0.005	16	-0.018	0		
S(5)	-0.018	16			-0.113	0
N(7)	-0.015	7	0.006	7		
N(8)	-0.138	7	-0.006	7		
N(9)	-0.095	7			0.010	7
N(10)	-0.093	7			-0.011	7
C(11)	-0.009	6	-0.007	6		
C(12)	0.016	6	-0.007	6		
C(13)	-0.006	6	0.006	6		
C(14)	-0.071	6	0.008	6		
C(15)	-0.058	6			-0.008	6
C(16)	0.004	6			-0.018	6
C(17)	0.046	6			0.016	6
C(18)	-0.021	6			0.011	6

Because of the ability of the dicyanoethylenedithiolato and other ethylenedithiolato ligands to stabilize unusual (formal) oxidation states of the chelated metal, it is of interest to construct some valence description of the molecular bonding. Except for the bond distances involving nickel and sulfur, the single valence-



Table 5. Average distances and angles in the mononegative (this investigation) and dinegative (EICG) ions  $\text{Ni}[\text{S}_2\text{C}_2(\text{CN})_2]_2^z$

Atomic labels are those used in this paper. Values in parentheses are standard deviations of the averages.

Distances (Å)	z = 1 -	z = 2 -
Ni-S	2.146(1)	2.160(5)
S-C	1.714 (4)	1.750 (10)
N-C	1.140 (6)	1.13 (1)
C(11)-C(12)	1.430 (5)	1.43 (1)
C(12)-C(13)	1.356 (7)	1.30 (2)

Angles (°)	z = 1 -	z = 2 -
S(2)-Ni-S(4)	92.4 (1)	91.7 (5)
Ni-S-C	103.3 (3)	103.0 (5)
S(2)-C(12)-C(13)	120.6 (5)	121.5 (10)
C(11)-C(12)-C(13)	121.9 (6)	122.0 (10)
N(7)-C(11)-C(12)	178.4 (6)	178.0 (10)

bond structure given in (I) is quite adequate. The  $C_{sp^2}-C_{sp}$  single bond length of  $1.430 \pm 0.005$  Å agrees well with the average ( $1.439 \pm 0.01$  Å) of several recent accurate measurements (Dewar & Schmeisling, 1960). The  $C_{sp^2}-C_{sp^2}$  double bond is only slightly longer ( $1.356 \pm 0.007$  Å) than the mean given by Dewar & Schmeisling (1.338 Å) and is nearly the same as that (1.353 Å) in propylene (Lide & Mann, 1957). The C-N triple bond ( $1.140 \pm 0.005$  Å) agrees reasonably with the average ( $1.158 \pm 0.002$  Å) of several accurate measurements on cyanohalides (Sutton, 1958).

Both the mean C-S distance of  $1.714 \pm 0.004$  Å and the mean Ni-S distance of  $2.146 \pm 0.001$  Å are considerably shorter than the sums of covalent radii (1.81 and 2.24 Å, respectively) given by Pauling (1960). However, because of recent emphasis (Dewar & Schmeisling, 1960, for example) on the fairly large dependence of bond lengths on hybridization as well as on bond order, it is well to ask what part of this shortening is due to rehybridization of carbon and sulfur from the  $sp^3$  states used as reference. The known difference of 0.04 Å between  $C_{sp^3}$  and  $C_{sp^2}$  radii would indicate an expected  $C_{sp^2}-S_{sp^3}$  length of 1.77 Å. It is difficult to specify the hybridization state of sulfur in this compound, but

it probably approaches  $sp^2$ , and a still shorter bond length would thus be expected, perhaps 1.74-1.73 Å. Such a sulphur would have a radius of about 1.00 Å; a Ni-S distance of 2.20 Å would be expected. Because the observed Ni-S and S-C distances are shorter than these proposed standards, some multiple bonding involving sulfur doubtless is present. Inadequate reference values, however, preclude any more distinct statement.

Fragments of the triphenylmethylphosphonium ion are of the expected geometry: Phenyl rings are planar with a mean C-C distance of 1.381 Å and the phosphorus and methyl carbon atoms are tetrahedral within experimental error. Some individual bond distances and angles are given in Table 6. The C-C phenyl distances all are between 1.353 Å and 1.392 Å, with a r.m.s. deviation from the mean of 0.009 Å. All PCC angles lie between 118.1° and 121.6°. Least-squares planes I-III through the phosphorus and carbon atoms, calculated with weights of 17 for P and 6 for C, are given in Table 7.

Table 6. Some interatomic distances and angles in the cation

Distances		Angles	
P(6)-C(19)	1.786 Å	C(19)-P(6)-C(20)	109.2°
C(20)	1.800	19	26
C(26)	1.798	19	32
C(32)	1.800	20	26
C(19)-H(53)	0.93	20	32
H(54)	0.95	26	32
H(55)	1.08		

The P-C<sub>methyl</sub> distance is 1.786 Å; the other three P-C bonds average  $1.799 \pm 0.006$  Å. These values are considerably shorter than the value of  $1.87 \pm 0.02$  Å found in trimethylphosphine (Sutton, 1958) and somewhat shorter than the average of  $1.835 \pm 0.03$  Å in  $[(\text{CH}_3)_2\text{PBH}_2]_3$  (Sutton, 1958). The small number of measured PC bond distances renders Sutton's reference values somewhat uncertain; it seems probable that 1.83 Å is nearly correct for  $P_{sp^3}-C_{sp^3}$  and 1.80 Å for  $P_{sp^3}-C_{sp^2}$ .

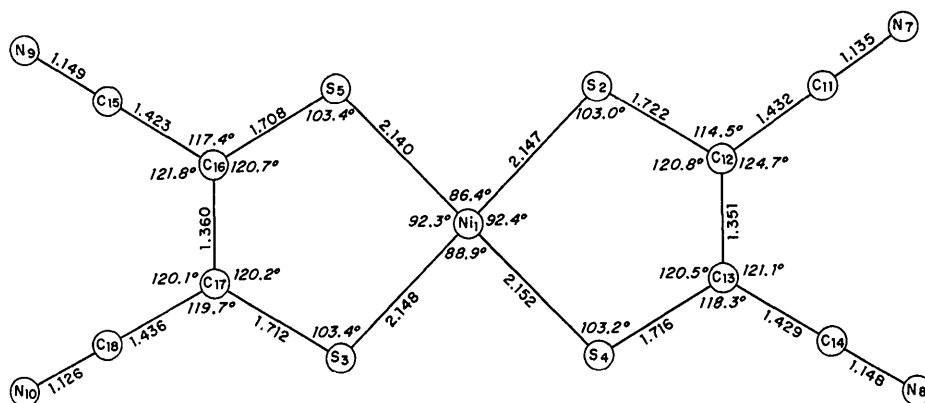


Fig. 1. Bond distances and angles in the anion.

Table 7. Least-squares planes defined by the phosphorus atom and phenyl rings

Coordinate system as in Table 4

Plane I; C(20)–C(25):  
 $-0.28661m - 0.87592n - 0.38811p = 0.5711$

Plane II; C(26)–C(31):  
 $-0.31005m + 0.84335n - 0.43890p = 0.2089$

Plane III; C(32)–C(37):  
 $0.71780m + 0.41158n - 0.56157p = 6.3198$

Atom	$\Delta_I$	Atom	$\Delta_{II}$	Atom	$\Delta_{III}$
P(6)	-0.000 Å	P(6)	-0.006	P(6)	-0.001
C(20)	-0.006	C(26)	0.006	C(32)	-0.004
C(21)	0.004	C(27)	0.007	C(33)	0.003
C(22)	0.004	C(28)	0.010	C(34)	0.008
C(23)	-0.007	C(29)	-0.025	C(35)	-0.014
C(24)	0.001	C(30)	0.002	C(36)	0.006
C(25)	0.006	C(31)	0.016	C(37)	0.005

A projection of the  $P(C_6H_5)_3CH_3^+$  ion down the  $C_{methyl}-P$  bond is given in Fig. 2. The configuration is quite different from a propeller shape that might be expected, the methyl carbon atom being quite close ( $-0.045$  Å) to the plane defined by P(6) and ring II. The methyl group is probably forced by its proximity to a hydrogen of ring II to take a staggered configuration about the PC bond; methyl hydrogen (55) is only 0.02 Å from plane II. The remaining phenyl rings show only slight distortion from a symmetrical propeller model.

#### Intermolecular packing

Despite electrostatic attraction, the two ionic components of this structure separate to a considerable extent. By far the largest part of the surface of each anion is bounded by other anions. Similarly, the phenyl rings II of the cations form columns running through the structure parallel to  $b$  and have as chief neighbors methyl and phenyl groups. It seems likely that interanionic spin-spin coupling, together with weak phenyl-phenyl interactions, are primarily responsible for this packing arrangement. Certainly, approximations to columnar packing of phenyl rings are fairly frequently encountered.

Interplanar separations along the stack of phenyl groups shown in Fig. 3 are 3.473 Å (II–II') and 3.619 Å (II–II''). In the figure, the sphere labelled  $A$  represents

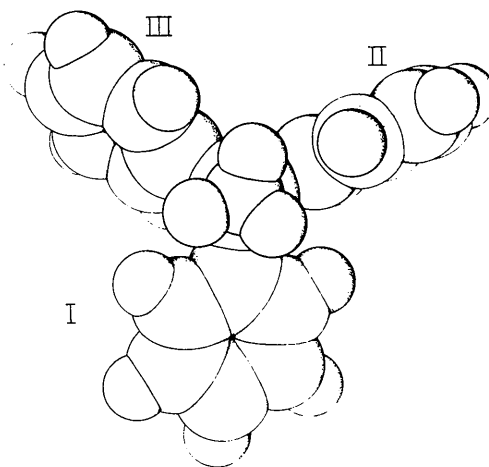


Fig. 2. The cation viewed along the  $P-C_{methyl}$  axis. Rings II and III, together with a centrally related pair, form a well-packed dimer which in turn is part of the anionic column.

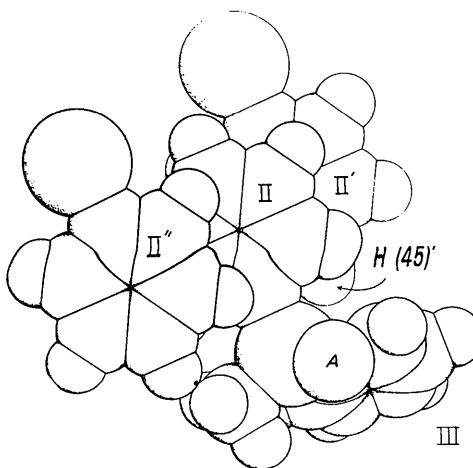


Fig. 3 A portion of the stack of cations, viewed along a normal of ring II. Ring I is symbolized by the sphere  $A$ .

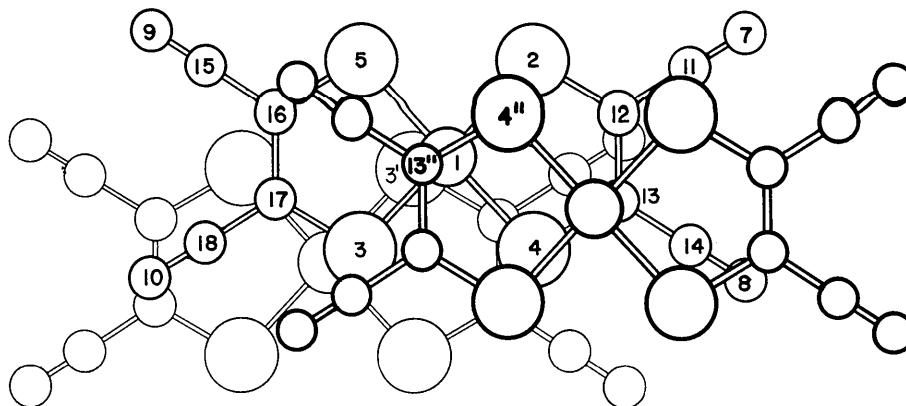


Fig. 4. Stacking of the anions, viewed along a normal to their least-squares planes.

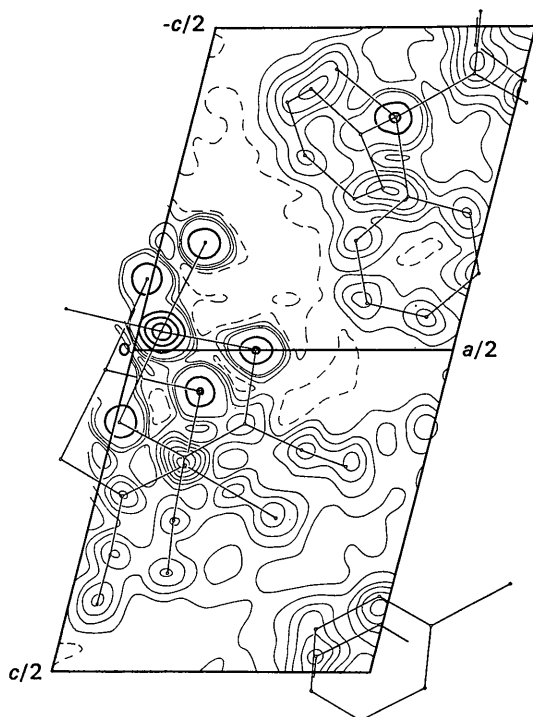


Fig. 5. The [010] electron density projection. Contours begin at zero (dashed) and are spaced at  $1 \text{ e.}\text{\AA}^{-3}$  intervals except for heavy lines, which represent  $5 \text{ e.}\text{\AA}^{-3}$  intervals.

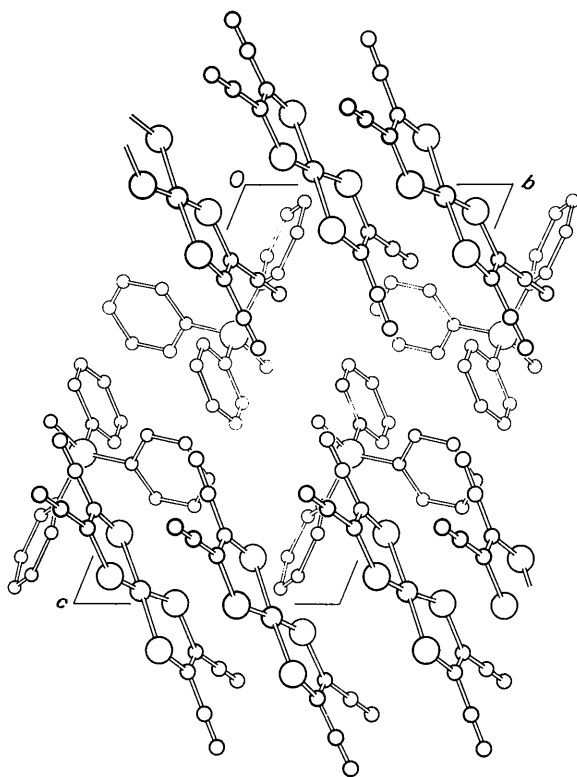


Fig. 6. A view of the structure along [100].

phenyl ring I of the unprimed molecule, and only phosphorus atoms attached to rings II' and II'' are shown for clarity. Centers of symmetry lie between each pair of neighboring rings. In addition to face-to-face packing of phenyl rings, the column of cations shows another feature of phenyl packing, the nesting of a hydrogen atom in the center of a neighboring ring. H(45') attached *para* to phosphorus is symmetrically bounded by the six carbon atoms of ring III as can be seen in Fig. 3. These C...H distances are 3.00, 3.02, 3.07, 3.12, 3.08, and 3.02 Å, all near the sum of van der Waals radii (2.9 Å; Pauling, 1960).

Fig. 4 shows the immediate neighborhood of an anion and sheds light on the magnetic behavior of this salt. Direct Ni-Ni bonding at the observed distances of 4.40 Å and 4.45 Å is clearly ruled out, leaving Ni-S...Ni as the most direct pathway for spin transmission. Weiher, Melby & Benson (1964) using magnetic studies are able to probe the coupling more closely and state that the interaction is best described as a coupling of the radicals in pairs. Examination of Fig. 4 in the light of this suggestion makes it apparent that the central and lower ions could be a coupled pair, the upper ion being half of an adjacent pair. Assuming that sulfur is the intermediary for spin transmission, one sees that S(3') in the lower anion is clearly in a more favourable position than S(4'') in the upper anion. It is both closer to (3.591 Å *vs* 3.708 Å) and, with respect to the plane normal, more nearly superimposed on Ni(1) than S(4''). Although the lack of planarity of the anion makes somewhat ambiguous the definition of interplanar separations, the spacing of the least-squares planes (3.412 Å between the unprimed and singly-primed planes and 3.555 Å between the unprimed and doubly primed planes) also supports this pairing assignment.

In addition to the probably eustructural contacts (those near the minimum of two-atom van der Waals potentials) within columns described above, other van der Waals contacts were examined. No holes exist in the structure other than a certain looseness at the extremes of the anion which probably results in its observed non-planarity; the only short contacts are between nitrogen atoms and various hydrogen atoms. Three N...H contacts are shorter than the sum of van der Waals radii (2.7 Å; Pauling, 1960). These are N(7)-2H(47) at 2.53 Å, N(9)-H(55) at 2.52 Å, and N(10)-3H(38) at 2.51 Å. All considerably exceed the N...H hydrogen bond length of about 2.2 Å in solid HCN (Pauling, 1960, p. 459). The italic figures preceding atomic labels above indicate symmetry-related atoms: 2 denotes the symmetry operation  $(1-x, 1-y, -z)$ , and 3 denotes  $(-1+x, y, z)$ . Nitrogen atom (8), which deviates most from the least-squares plane, and also C(14) have no close neighbors on one side but are closely bounded on the other (see Figs. 4 and 5). To a lesser extent the same situation is found at N(9). Although very close contacts and therefore repulsion are absent, it is likely that looseness on one side coupled with the large thermal

motion (maximum principal axes of 10–14 Å<sup>2</sup>) results in mean positions for these atoms which are somewhat displaced toward the more distant neighbors. Because of the known presence of absorption errors, no detailed analysis of thermal motion was made. The ellipsoids are reasonable in size and orientation, however, varying from nearly spherical for Ni(1) (3.3 × 3.7 × 3.9) and P(6) (3.0 × 3.6 × 4.2) to highly elongated for nitrogen atoms [4.4 × 6.1 × 14.4 for N(9)] and *para* carbon atoms [3.5 × 4.5 × 10.3 for C(35)].

Thanks are due to Dr L.R. Melby for pointing out the interesting features of this material and for supplying crystals. The author is further grateful to Drs Weiher, Melby, and Benson for a copy of their paper prior to publication and for discussions concerning the magnetic behavior of this and similar materials. Dr Charles T. Prewitt, Mr George McCowan, and Mr Dan Usavage worked closely with the author in the design and construction of the precision Weissenberg camera described.

### References

- CAVALCA, L., NARDELLI, M. & FAVA, G. (1962). *Acta Cryst.* **15**, 1139.  
 DAVISON, A., EDELSTEIN, N., HOLM, R. H. & MAKI, A. H. (1963). *J. Amer. Chem. Soc.* **85**, 2029.  
 DEWAR, M. J. S. & SCHMEISLING, H. N. (1960). *Tetrahedron*, **11**, 96.  
 EISENBERG, R., IBERS, J., CLARK, R. J. H. & GRAY, H. B. (1964). *J. Amer. Chem. Soc.* **86**, 113.  
 FREEMAN, A. J. (1959). *Acta Cryst.* **12**, 261.  
 HOERNI, J. A. & IBERS, J. A. (1954). *Acta Cryst.* **7**, 744.  
 LIDE, D. R., JR. & MANN, D. E. (1957). *J. Chem. Phys.* **27**, 868.  
 MCWEENY, R. (1951). *Acta Cryst.* **4**, 513.  
 PARRISH, W. (1960). *Acta Cryst.* **13**, 838.  
 PAULING, L. (1960). *Nature of the Chemical Bond*, 3rd Ed. Ithaca: Cornell Univ. Press.  
 SUTTON, L. E. (1958). *Tables of Interatomic Distances and Configurations in Molecules and Ions*. London: The Chemical Society.  
 WEIHER, J. F., MELBY, L. R. & BENSON, R. E. (1964). *J. Amer. Chem. Soc.* **86**, 4329.

*Acta Cryst.* (1966). **20**, 118

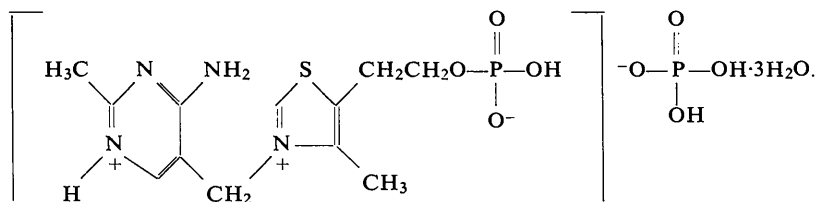
## The Crystal and Molecular Structure of Hydrolyzed Cocarboxylase\*

BY ISABELLA L. KARLE AND KATHLEEN BRITTS

*U.S. Naval Research Laboratory, Washington, D.C. 20390, U.S.A.*

(Received 29 April 1965)

A material thought to be cocarboxylase was actually found to be hydrolyzed cocarboxylase with the formula



It crystallizes in space group *P*1 with two molecules in the unit cell and the following unit-cell parameters:

$$\begin{array}{lll} a = 8.75 \text{ \AA} & b = 10.10 \text{ \AA} & c = 13.25 \text{ \AA} \\ \alpha = 101^\circ 53' & \beta = 108^\circ 54' & \gamma = 98^\circ 44' \end{array}$$

The parameters of the organic portion of the molecule are similar to those found in vitamin B<sub>1</sub>. The phosphate groups are hydrogen bonded to other phosphate groups and to the water molecules. Only the amino group and the adjacent nitrogen atom of the organic portion are involved in hydrogen bonding. The extra proton was found to be on the nitrogen atom opposite the amino group, as in vitamin B<sub>1</sub>, but it does not appear to be involved in any hydrogen bonding.

The structure was solved by obtaining phases directly from the structure factor magnitudes by means of the symbolic addition procedure.

### Introduction

Cocarboxylase, the pyrophosphoric acid ester of vitamin B<sub>1</sub>, plays a vitally important role in metabolic pro-

cesses in the form of biochemical decarboxylation of many  $\alpha$ -keto acids. It may be obtained naturally from yeast or rice polishings but is more readily produced synthetically (Weijlard & Tauber, 1938).

The structural formula for cocarboxylase is:

\* Presented at the February, 1965, meeting of the American Crystallographic Association.